Supplement of Geosci. Model Dev., 18, 10119–10142, 2025
https://doi.org/10.5194/gmd-18-10119-2025-supplement

Geoscientific Model Development
Open Access
EGU

Supplement of

Incorporation of lumped IVOC emissions into the ORACLE model (V1.1): a multi-product framework for assessing global SOA formation from internal combustion engines

Susanne M. C. Scholz et al.

Correspondence to: Alexandra P. Tsimpidi (a.tsimpidi@fz-juelich.de)

Table S1: Statistical evaluation of ORACLE-IVOC and ORACLE-base results for total SOA against global AMS datasets with PMF analysis compiled by Tsimpidi et al. (2025) from campaigns conducted in spring, summer and autumn during 2011–2020. To assess the models' performance, the mean absolute gross error (MAGE), mean bias (MB), normalized mean error (NME), normalized mean bias (NMB), and the root mean square error (RMSE) are used.

Region	Model	No. of datasets	Mean observed (μg m^{-3})	Mean predicted (μg m^{-3})	MAGE (μg m^{-3})	MB (μg m^{-3})	NME (%)	**NMB** (%)	RMSE (μg m^{-3})
Global	**Oracle-IVOC**	200	7.07	2.77	4.7	-4.3	66.47	-60.79	6.81
	Oracle-base			2.62	4.82	-4.45	68.14	-62.92	6.93
Europe	**Oracle-IVOC**	46	3.07	1.34	1.9	-1.73	61.93	-56.43	2.62
	Oracle-base			1.29	1.94	-1.78	63.14	-58.1	2.66
North-America	**Oracle-IVOC**	35	3.93	2.38	2.22	-1.55	56.52	-39.48	2.85
	Oracle-base			2.3	2.27	-1.63	57.68	-41.36	2.9
Eastern Asia	**Oracle-IVOC**	90	9.77	3.08	6.87	-6.68	70.32	-68.42	8.58
	Oracle-base			2.86	7.06	-6.91	72.32	-70.71	8.75

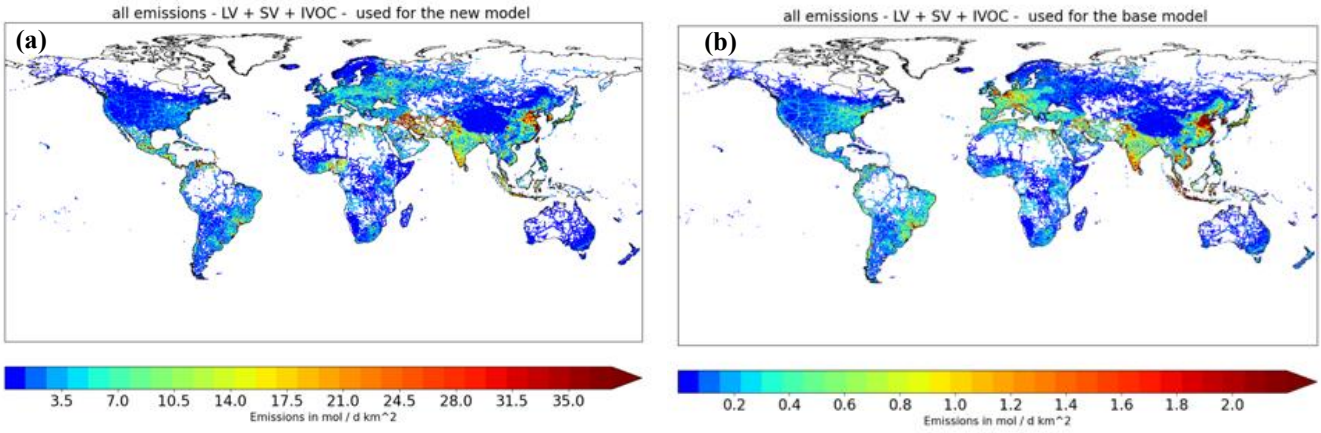

Figure S1: All primary emissions (LVOC+SVOC+IVOC) used for a) the lumped species simulation in ORACLE-IVOC and (b) the ORACLE-base simulation. In both cases, LVOC and SVOC taken from the OC inventory with proportions of 0.1 and 0.9, respectively. For (a), IVOC are considered with individual IVOC/NMVOC emission factors from both the gasoline and diesel NMVOC inventories, for (b), IVOC are approximated with 1.5 times the emissions from the OC inventory.

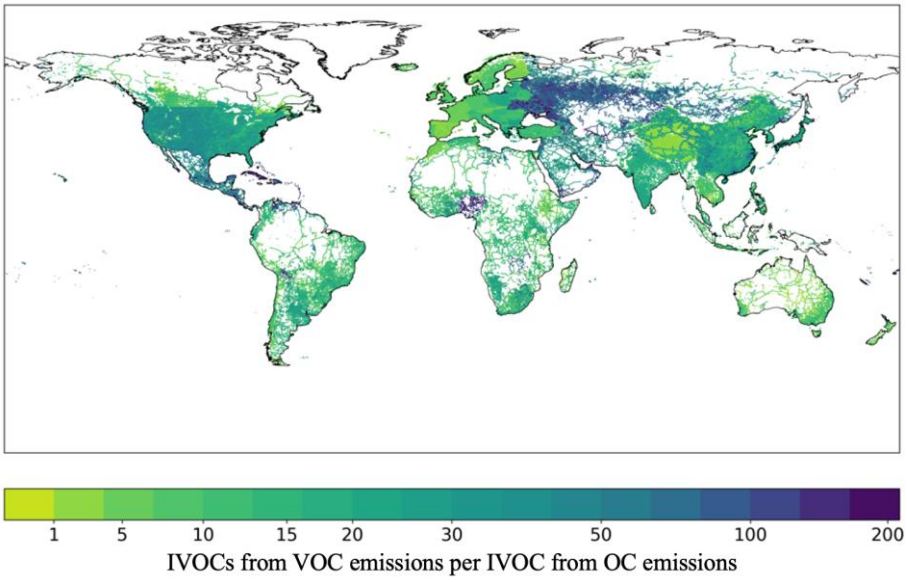

Figure S2: Ratio of IVOC emissions in mol d^{-1} km^{-2} from diesel and gasoline vehicles derived from VOC emissions (as in ORACLE-IVOC) to IVOC emissions derived from 1.5×OC road transport emissions.

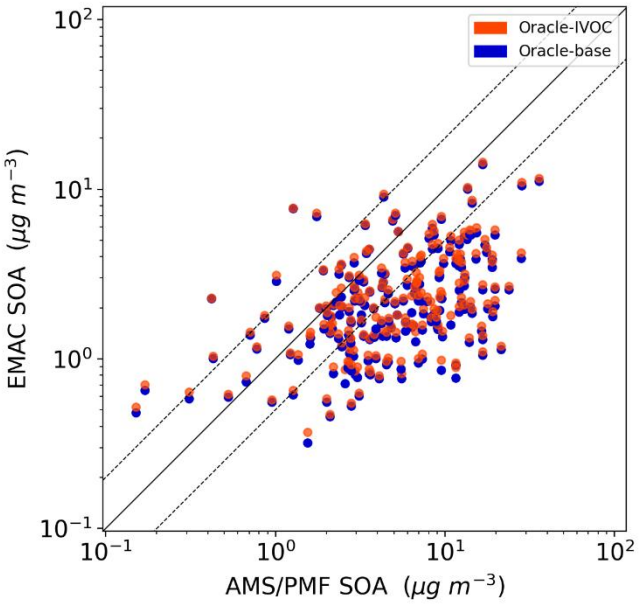

Figure S3: Scatter plot comparing ORACLE-base and ORACLE-IVOC results for total SOA against global AMS datasets with PMF analysis, compiled by Tsimpidi et al. (2025) from campaigns conducted in spring, summer and autumn during 2011–2020.

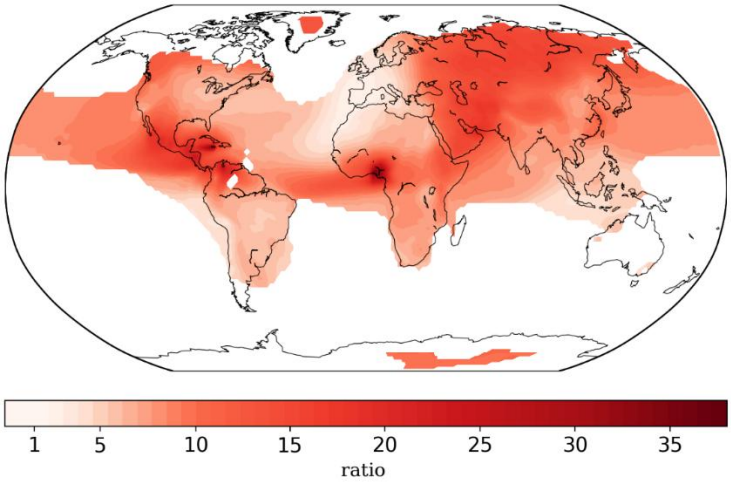

Figure S4: Road transport SOA-iv from ORACLE-IVOC as a multiple of SOA-iv from ORACLE-base. Locations where ORACLE-IVOC concentrations are below the 60th percentile are shown in white.

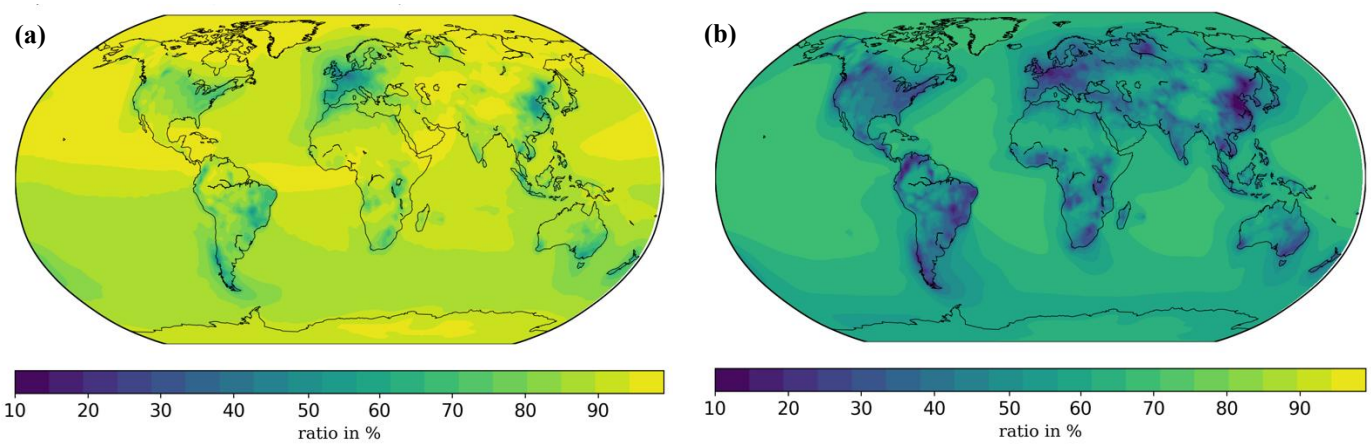

Figure S5: Ratio of modelled SOA-iv to total OA from road transport emissions as simulated with (a) ORACLE-IVOC and (b) ORACLE-base.

References

Tsimpidi, A. P., Scholz, S. M., Milousis, A., Mihalopoulos, N., and Karydis, V. A.: Aerosol Composition Trends during 2000–2020: In depth insights from model predictions and multiple worldwide observation datasets, EGUsphere, 2024, 1–66, https://doi.org/10.5194/acp-25-10183-2025, 2025.